International Journal of Applied Engineering Research ISSN 0973-4562 Volume 10, Number 22 (2015) pp 43097-43102

Effect of flux on microstructure and mechanical properties of super martensitic stainless steel using Activated Tungsten Inert Gas welding process

[*1]M.Chellappan,

[1]*Department of Mechanical Engineering, Dhanalakshmi Srinivasan Engineering college Perambalur-621212, Tamilnadu, India.*

[2]K.Lingadurai

[2]*Department of Mechanical Engineering, University College of Engineering Dindigul-624622, Tamilnadu, India.*

[3]P. Sathiya

[3]*Department of Production Engineering, National Institute of Technology Tiruchirappalli-620015, Tamilnadu, India*

Abstract
The super martensitic stainless steel (SMSS) is an economical alternative to the traditional carbon steel and/or duplex stainless steel. In the present study, microstructure and mechanical properties of AISI 410S SMSS, A-TIG welded joints were investigated. For this purpose, activated tungsten inert gas welding (A-TIG) was used with different fluxes namely SiO_2, ZnO and 50% SiO_2 and 50% ZnO. The microstructure investigation was carried out with optical microscope. The phases present in the welds were analyzed by image analysis software. The results of hardness tests revealed that the hardness values are low in weld and base metal compared to the HAZ region.

Keywords: super martensitic stainless steel; bead on plate welding; Microstructure; Mechanical properties.

1. Introduction

Supermartensitic stainless steels (SMSS) are best alternatives to high-strength low-alloy (HSLA) steels mainly in applications related to the gasoline industry [1, 2]. Welding of SMSS plays a crucial role in fabricated components, influencing their toughness, weldability, and resistance to sulfide stress cracking. SMSS are developed from classic martensitic stainless steels (11-14% Cr), reducing C content to enhance weldability and corrosion resistance and adding Ni to promote a free-ferrite structure and Mo [3, 4], which also improves corrosion resistance [5, 6].The weld metal microstructure of SMSS is influenced by the weld metal composition and welding procedure type. These SMSS also consist of martensite and variable amount of austenite (up to 30%) and ferrite (up to 10%), with different morphologies [7].The effect of the different heat treatment on microstructures and mechanical properties of 13 Cr SMSS investigated. They found that, after quenching, the material has the lath martensites mixed with a small amount of retained austenite. The quenching temperatures increase the original austenite grain size and lath martensite become thicker [8].The effect of different heat treatment on the revised austenite in 15 Cr super austenite martensitic stainless steel studied. The results indicated that the microstructure of the steel is composed of tempered martensite and diffused revised austenite after quenching at 1050^0C and tempering from 550 to 750^0C.The size and volume fraction of revised austenite decrease when the tempering temperature is above 700^0C [9].
Ma et al., [10] studied the effect of nitrogen on microstructure and mechanical properties of 16 Cr SMSS. They found that, 0.1% N addition to 16%Cr5%Ni1%Mo martensitic stainless steel offers good strength properties and decreased ductility and toughness after tempering due to the severe precipitation of Cr_2N. Tempering treatment above 550^oC is undesirable for high nitrogen alloyed 16Cr5Ni1Mo martensitic stainless steel to achieve good combined mechanical properties. Ma et al., [11] investigated the effect of high amount of vanadium (0.09 wt%) and low amount of niobium (0.025 wt%) along with high amount of nitrogen (0.06 wt%) in SMSS on the microstructure and mechanical properties of a normalized and tempered commercial SMSS. They found that the Cr rich precipitates can be suppressed by lowering the nitrogen content and adding niobium, and the mechanical properties and resistance to pitting corrosion can be significantly improved. A systematic approach made to maximize the all weld metal toughness by the way of microstructural modification by means of different post weld heat treatments of SMSS. The Ar-18%CO_2 shielding gas has a lower toughness and ductility, and higher strength and hardness were obtained when compared to the Ar-5%He.Postweld heat treatment (PWHT) is usually necessary to adjust weldment properties [12]. Based on microstructural evolution as-welded condition of SMSS, high hardness and low toughness are obtained, due to the presence of untempered martensite [6, 13].In general, PWHTs involve single or double tempering treatments, promoting martensite tempering and formation of retained austenite, which results in lower hardness and higher toughness values [4, 14].
A variant of TIG known as A-TIG is gaining importance in the fabrication of power plant components worldwide [18]. In general, the flux used in the A-TIG process causes an inward flow of molten metal, steep temperature gradient and more

constricted arc, hence deeper penetration [19, 20]. Other attractive features of this process include high productivity, slag-free welding process, consumable—free process, less distortion, and a beneficial compressive residual stress after welding in grade 91 steel weld joints [15].The mixtures of fluxes are defused in the weld pool so as to produce sufficient amount of oxygen to reverse the flow of molten pool. Which is known as a reversed marangoni convection [16].This mechanism was considered as the main factor for controlling the fluid flow in the liquid weld pool, which transforms the outward flow of Marangoni convection into an inward flow. This mechanism allows a wide range of welding parameters to obtain a deeper and narrow weld pool [17]

The oxide flux SiO_2 cause an important increase in penetration on JIS SUS 304 stainless steel in A-TIG welding process [21, 22]. Using oxide fluxes of SiO_2, MoO_3, and Cr_2O_3 not only increased the penetration capability, but also improved the mechanical properties of grade 2205 duplex stainless steel in the A-TIG welding process [23].From the above discussions available in the literature, we observed that very limited attempts were made to investigate the effect of the different flux on GTAW of SMSS welds. Welding of SMSS plays a crucial role in fabricated components, influencing their toughness, weldability, and resistance to sulphide stress cracking.

In the present investigation an attempt has been made to find the effect of different activating flux namely SiO_2, ZnO and 50% SiO_2 + 50% ZnO in A-TIG welding of SMSS materials. The objective of the research is to study in detail the effect of different fluxes on bead on plate welds mechanical properties in terms of hardness and also to study the effect of the microstructural characterization of the welds.

2. Experimental Procedure:

2.1. Base metal and welding procedure

The chemical composition of the as-received base metal AISI 410 S SMSS is shown in Table 1.

TABLE.1 Base metal chemical composition (wt.%)

Materials	C	Si	Mn	P	S	Cr	Mo	Ni	Cu	Ti	Fe
Base metal	0.04	0.41	0.62	0.02	0.01	12.21	0.10	0.38	0.21	0.003	Bal

Before welding, using wire-cut Electrical Discharge Machining (EDM) the base metal plates were machined to have the dimensions of 100X50X6 mm. Welding was carried out using electrode negative A-TIG with a 2% thoriated tungsten electrode of 2.4 mm diameter. A-TIG welding was carried out on these plates using a fixture to hold the parts in proper alignment. The process parameters are presented in Table 2.

TABLE.2 Welding process parameters

Current (Amps)	Voltage (Volts)	Travel speed (mm/min)	Gas flow rate (lpm)
170	27	60	14

The photograph view of the bead on plate welds are presented in Figure 1.

Fig.1.Photograph view of the bead on plate welds

2.2. Metallurgical and mechanical characterization of the weldments

After completing the welding, the welds were characterized to determine any weld defects by radiography technique. Ensuing to the radiography results, the weld samples were sliced into coupons of various dimensions to conduct metallurgical and mechanical tests. Microstructure studies were performed at various zones of the weld zones using Optical Microscopy (OM). The weld zones were polished as per the standard metallographic procedures including polishing with emery sheets of SiC with grit size varying from 200 to 1200 and followed by disc polishing using alumina paste and distilled water to obtain a mirror finish.

Electrolytic etching (Villella's Reagent-5 ml HCl+ 1gm Picric Acid + 100 ml Methanol; 6 V DC supply; current density of 1 A/C m^2) was employed to examine the microstructures. Microhardness studies were carried out on the SMSS weldments across the longitudinal direction of the weldments by keeping weld as center using Vicker's microhardness tester. A standard load of 0.5 kg was applied for a dwell period of 15 s and the measurements were carried out at regular intervals of 0.25 mm across the traverse section of the weld region.

3. Results and Discussions

3.1 Macrostructure of the weld region.

The macrostructure of the different flux coated TIG welds are presented in Figure 2.Figure 2(a) shows SiO_2 flux produce deeper penetration than the other two fluxes. The depth of penetration was increased due to the increased oxygen content which can be explained by Reversed Marangoni convection. This theory relates the increase in penetration depth to the direction of fluid flow. The surface tension temperature coefficient is a factor in determining direction of molten fluid flow. The shallow penetration in TIG welding was because of the negative surface tension gradient and centrifugal convection movement. The centripetal convection movement which results in increased penetration depth in A-TIG welding was due to the addition of oxide flux, which changes the surface tension gradient sign by the inversion of convection current. The improper interaction between the flux composition and base material composition might be the cause for lower depth of penetration.

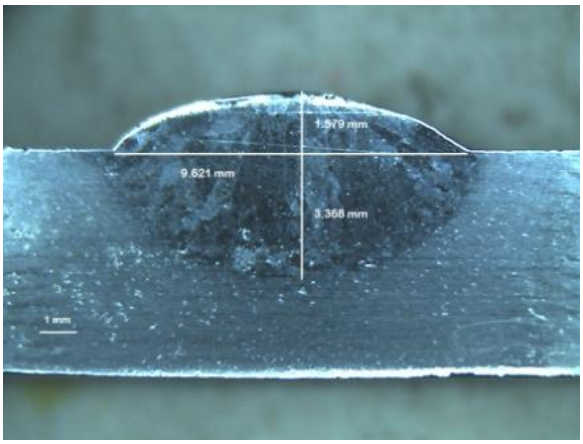

(a) SiO_2

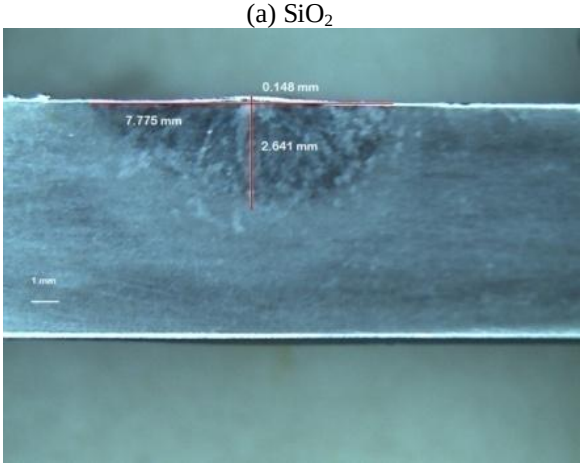

(b) ZnO

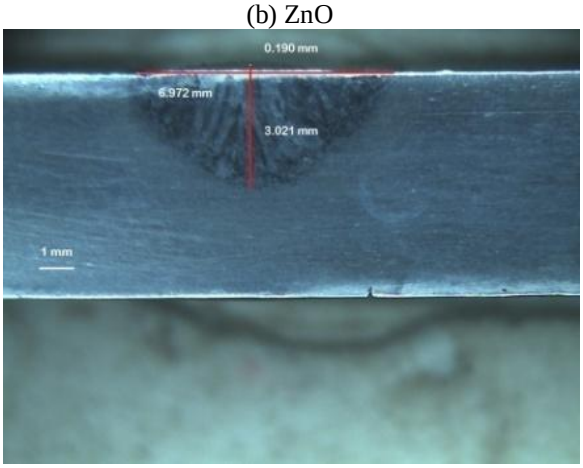

(c) 50% SiO_2 and 50% ZnO

Fig.2. (a-c) Macrograph of the bead on plate weldments.

3.2 Microstructure analysis

The optical image of the base metal, Figure 3(a and b), in the as-received condition shows rolled, panacke structure with various grain size.The optical microstructure and phase mapping structure of the AISI 410 S SMSS is presented in Figure 3 (b).

Figure 3(a) shows clearly a well defined grain boundary region. The base material has an elongated grains of δ-ferrite and also streaks (like plates) of δ-ferrite and also randomly distributed globular particles of Cr_2C_3. Figure 3 (b) shows that the delta ferrite phase in the matrix of martensite is 46% and the alpha ferrite phase, appears to be elongated bands, is 44%.The weld metal and heat affected zone (HAZ) microstructures with different flux are presented in Figure 4 (a-c) and Figure 5 (a-c).

Figure 4 (a) shows martensite in a ferrite matrix, feather type of martensite is observed, but Cr_2C_3 evenly distributed in the matrix. Figure 4 (b) presents, precipitated particles are Cr_2 carbides which are evenly distributed in a matrix.Figure 4 (c), shows tree like structure dark etching martensite in a ferrite matrix along with globular particles are Cr_2 carbides.

Figure 5 (a and b) shows banded structure of ferrite along with randomly distributed carbides in certain amount of grain boundary carbides in the ferrite matrix.Figure 5 (c) shows equiaxed ferrite grains with carbides along the grain boundaries.The weld metal and HAZ microstructure were further analyzed by the phase analysis software and percentage of phases present in the weld and HAZ are presented in Table 3. Due to the higher heat input provided by the SiO_2 flux the formation of martensite has reduced and the higher cooling rate provided by the ZnO flux has led to the formation of martensite in higher amount in the weld as well as the HAZ region

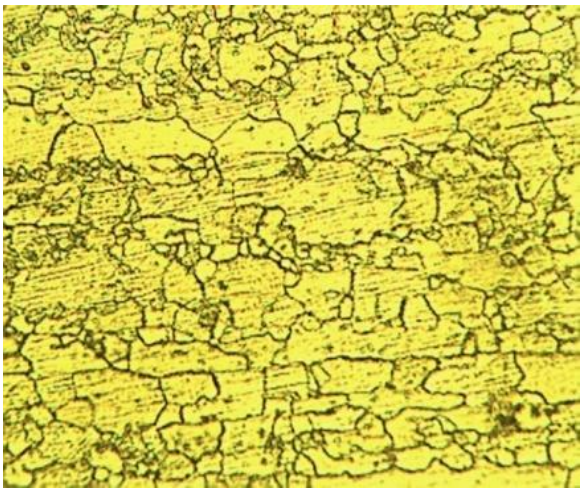

(a) Optical microstructure

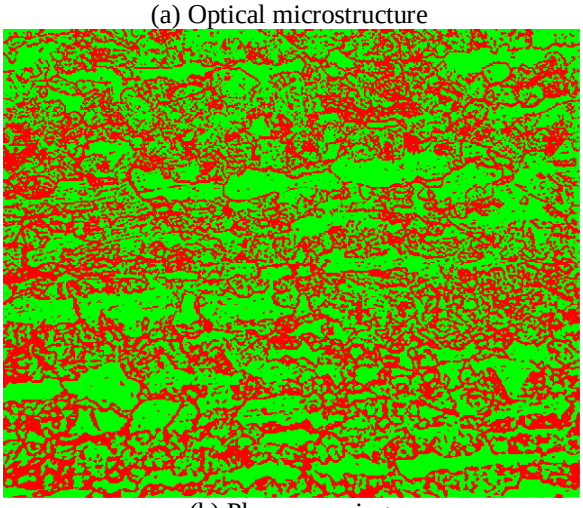

(b) Phase mapping

Fig.3.(a and b) Base material microstructures

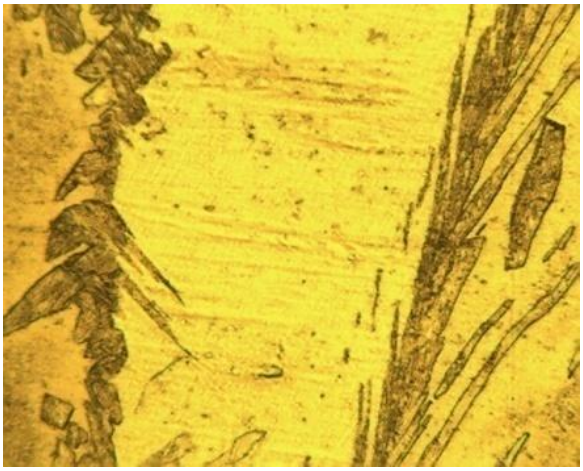

(a) SiO_2

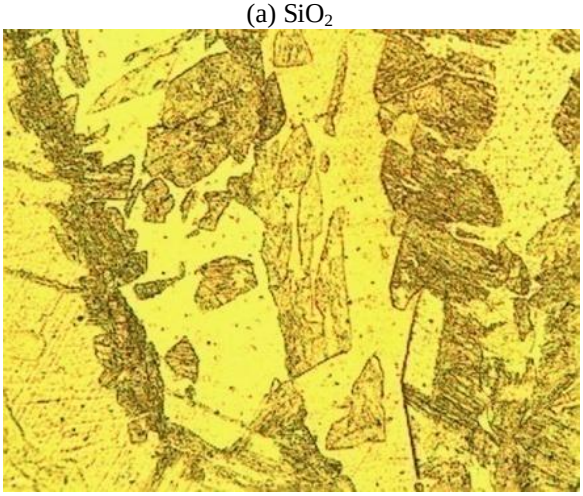

(b) ZnO

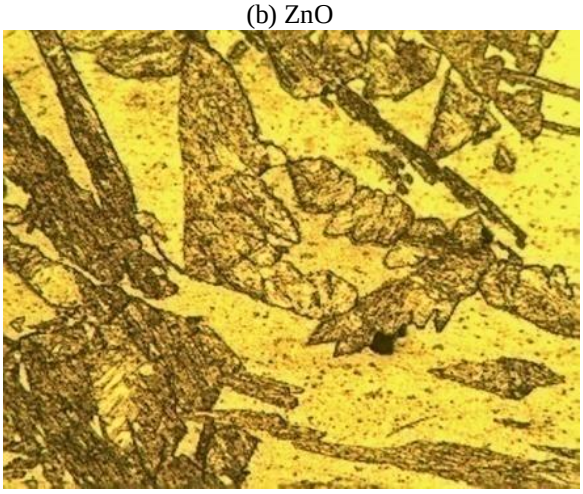

(c) 50% SiO_2 and 50% ZnO

Fig.4.(a-c)as-weld metal microstructures

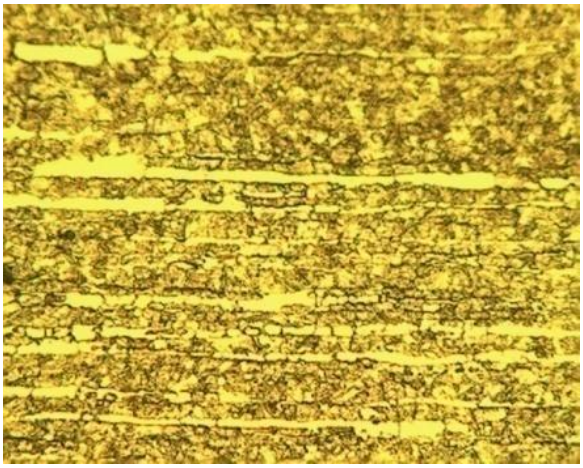

(a) SiO_2

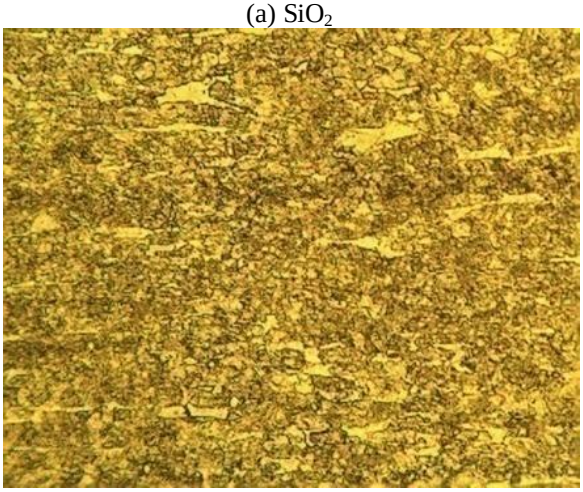

(b) ZnO

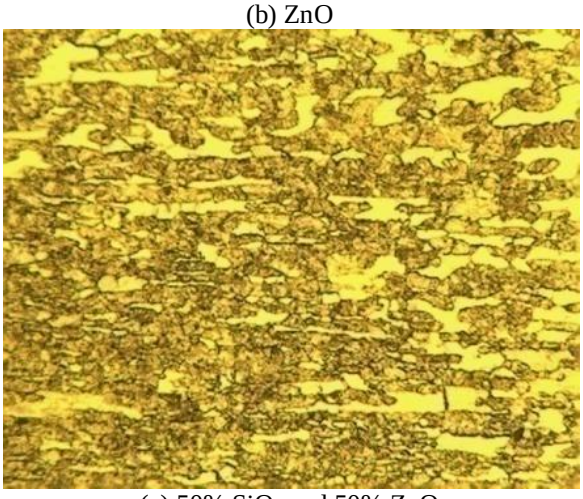

(c) 50% SiO_2 and 50% ZnO

Fig.5. (a-c) HAZ microstructures

TABLE. 3 Areal fraction of phases present in the weld and HAZ

Flux	HAZ		Weld Metal	
	% of martensite	% of ferrite	% of martensite	% of ferrite
SiO_2	67	28.07	53.89	47.04
ZnO	73.5	26.5	55.63	45.3
50% SiO_2 and 50% ZnO	73.85	26.63	67.81	32.86

3.3 Mechanical properties

3.3.1 Hardness measurement:

The hardness measurements were carried out in different zones like base metal, HAZ and weld metal. In each zone five measurements were taken and their average values are presented in Table 4.

From Table 4 it is clear that the weld metal hardness values are lower when compared to the base metal and HAZ. The difference in microhardness of HAZ and weldments can be attributed to the differences in the grain size and also major constituents of the martensite phases presented in the HAZ region.

TABLE. 4 Average hardness values in different zones

Exp. No.	Base metal	HAZ	weld metal
SiO_2	283	314	257
ZnO	281	302	243
50% SiO_2 and 50% ZnO	286	293	224

4. Conclusions

The A-TIG welding was carried out on SMSS material with different flux and its combination and the mechanical and microstructural properties were studied. The following conclusions are made from the observations.

- SiO_2flux produces deeper penetration compared with other fluxes due to the increased amount of oxygen provided by the flux.
- The main mechanism for the increased depth of penetration was the reversed marangoni convection.
- The hardness values are low in weld and base metal compared to the HAZ region for all the weldments.
- The higher cooling rates provided by the ZnO flux has led to the formation of higher amount of martensite which would seriously degrade the strength of the joints.

References:

[1] Marshall, A. W., and Farrar, J. C. M. 1998. Welding of ferritic and martensitic 13%Cr steels.Preliminary report (draft 2). IIW Doc IX-H-422-98: 1 to 18.

[2] Farrar, J. C., and Marshall, A. W. 1998. Supermartensitic stainless steel — overview and weldability.IIW Doc No. IX-H 423-98: 1-3.

[3] Bilmes, P. D. 2000. Role of austentite on mechanical properties of soft martensitic stainless steel weld metals. PhD dissertation. La Plata, Argentina. Universidad Nacional de La Plata, Facultad de Ingeniería.

[4] Lippold, J. C., and Kotecki, D. J. 2005. *Welding Metallurgy and Weldability of Stainless Steels.*John Wiley & Sons, Inc.

[5] Karlsson, L., Rigdal, S., Sweden, G., Bruins, W., and Goldschmitz, M. 1999. Development of matching composition supermartensitic stainless steel welding consumables. *Svetsaren*No. 3: 3-7.

[6] Kvaale, P. E., and Olsen, S. 1999. Experience with supermartensitic stainless steels in flow line applications.*Stainless Steel Word*. The Hague, The Netherlands.

[7] Karlsson, L., Bruins, W., Gillenius, C., Rigdal, S., and Goldschmitz, M. 1999. Matching composition supermartensitic stainless steel welding consumables. *Supermartensitic StainlessSteels '99.*Brussels, Belgium.

[8] Liu Yu-rong, YE Dong, YONG Qi-long, SU Jie, ZHAO Kun-yu, JIANG Wen, Effect of heat treatment on microstructure and property of Cr 13 super martensitic stainless steel, Journal of iron and steel research, International, 2011, 18(11), 60-66.

[9] JIANG Wen, ZHAO Kun-yu, YE Dong, LI Jun, LI Zhi-dong, SU Jie, Effect of heat treatment on reverse austenite in Cr 15 super martensitic stainless steel, Journal of iron and steel research, International, 2013, 20(5), 61-65.

[10] X.P. Ma, L.J. Wang, B. Qin, C.M. Liu, S.V. Subramanian, Effect of N on microstructure and mechanical properties of 16Cr5Ni1Mo martensitic stainless steel, Materials and Design 34 (2012) 74-81.

[11] X.P. Ma, L.J. Wang, C.M. Liu, S.V. Subramanian, Microstructure and properties of 13Cr5Ni1Mo0.025Nb0.09V0.06N super martensitic stainless steel, Materials Science and Engineering A 539 (2012) 271-279.

[12] S. ZAPPA, H. G. SVOBODA, N. M. RAMINI DE RISSONE, E. S. SURIAN, AND L. A. DE VEDIA, Improving Supermartensitic Stainless Steel Weld Metal Toughness, Welding Journal, 2012, Vol. 91, 83s-90s.

[13] Zappa, S., Svoboda, H., Ramini de Rissone, M., Surian, E., and de Vedia, L. 2007. Effect of post weld heat treatment on the properties of a supermartensitic stainless steel deposited with tubular metal-cored wire. *Soldagem&Inspecão*12(2): 115-123.

[14] Bilmes, P. D., Llorente, C. L., and Solari, M. 1998. Effect of post weld heat treatment on the microstructure and mechanical behavior of 13Cr-4NiMoL and 13Cr-6NiMoL weld metals. *The 18th ASM Heat Treating Society Conference and Exposition.*Chicago, Ill.

[15] M. Sireesha, ShajuK Albert, and S. Sundaresan, Microstructure and Mechanical Properties of Fusion Zones in Modified 9Cr-1Mo Steel, J. Mater. Eng. Perform. 2001, 10(3), p 320-330

[16] Kou S. Welding metallurgy.2nd ed. Wiley-Interscience Publishers; 2003.p.116-7.

[17] Dongjie Li, Shanping Lu*, Wenchao Dong, Dianzhong Li, Yiyi Li. Study of the law between the weld pool shape variations with the welding parameters under two TIG processes Journal of Materials Processing Technology 212(2012) 128-136.

[18] V. Maduraimuthu, M. Vasudevan, V. Muthupandi, A.K. Bhaduri, and T. Jayakumar, Study of the Effect

of Activated Flux on the Microstructure and Mechanical Properties of Mod. 9Cr-1Mo Steel, Metall, Mater. Trans. B, 2012, 43(1), p 123-132

[19] S. Kou, Active Flux GTAW, Welding Metallurgy, 2nd Ed., Wiley, 2003, p 116-117

[20] S.N. Shyu, H.Y. Huang, K.H. Tseng, and C.P. Chou, Study of the Performance of Stainless Steel A-TIG Welds, J. Mater. Eng. Perform., 2008, 17(2), p 193-201

[21] H.Y. Huang, S.W. Shyu, K.H. Tseng, and C.P. Chou, Study of the Process Parameters on Austenitic Stainless Steel by TIG-Flux Welding, J. Mater. Sci. Technol., 2006, 22(3), p 367-374

[22] C.L. Yang, S.B. Lin, F.Y. Liu, L. Wu, and Q.T. Zhang, Research on the Mechanism of Penetration Increase by Flux in A-TIG Welding, J.Mater. Sci. Technol., 2003, 19(1), p 225-227

[23] T.S. Chern, K.H. Tseng, and H.L. Tsai, Study of the Characteristics of Duplex Stainless Steel Activated Tungsten Inert Gas Welds, Mater.Des., 2011, 32, p 255-263